Korean Journal of Geomatics
Vol. 5, No. 1 / December 2005
pp. 35~42

Surface-based Geometric Registration of Aerial Images and LIDAR Data

Impyeong LEE*, Seong Joon KIM and Yunsoo CHOI*****

Abstract

Precise geometric registration is required in multi-source data fusion process to obtain synergistic results successfully. However, most of the previous studies focus on the assumption of perfect registration or registration in a limited local area with intuitively derived simple geometric model. In this study, therefore, we developed a robust method for geometric registration based on a systematic model that is derived from the geometry associated with the data acquisition processes. The key concept of the proposed approach is to utilize smooth planar patches extracted from LIDAR data as control surfaces to adjust exterior orientation parameters of the aerial images. Registration of the simulated LIDAR data and aerial images was performed. The experimental results show that the RMS value of the geometric discrepancies between two data sets is decreased to less than ±0.30 m after applying suggested registration method.

Keywords : *geometric registration, aerial images, LIDAR, exterior orientation, planar patches*

1. Introduction

In many photogrammetric and remote sensing applications, data fusion of aerial images and LIDAR data is thought to produce more reliable results because of their characteristics complementary to each other (Schenk and Csatho, 2002). Such successful results from data fusion can be possible only if the data sets are geometrically registered in a sufficient degree of precision, however (Habib and Schenk, 1999; Postolov et. al. 1999; Habib et. al. 2004)

In the previous studies on data fusion, many researchers just simply assumed almost perfect registration that is not true in reality or registered them in only a small local area using a simple intuitive model. In this study, we thus attempted to develop a robust method for geometric registration using a systematic model derived from the geometry associated with the data acquisition processes. The core of this method is to utilize smooth planar patches extracted from LIDAR data as control surfaces without any ground control point to adjust the exterior orientation parameters of aerial images.

2. Methodology

The registration process consists of three fundamental steps, that is, generating registration primitives, finding the correspondence between the primitives, and adjusting the exterior orientation parameters. Each step is described in the following subsections.

2.1 Generating Registration Primitives

Registration primitives are the geometric features that we extract from two different data sets and use to register them, for examples, points, lines, and surface patches. The primary features extracted from images are the conjugate points, from which the three-dimensional points could be derived if the exterior orientation parameters of each image are given. As the corresponding features extracted from LIDAR data, planar surface patches are proposed. These patches can be segmented from the three-dimensional points obtained by a LIDAR system. Each patch is represented with its plane parameters and boundary. The original points cannot be used as the registration primitives since it is generally not practical to find the

*Dept. of Geoinformatics, The University of Seoul, Seoul, Korea (E-mail : iplee@uos.ac.kr)
**Dept. of Geoinformatics, The University of Seoul, Seoul, Korea (E-mail : sinus7953@uos.ac.kr)
***Dept. of Geoinformatics, The University of Seoul, Seoul, Korea (E-mail : choiys@uos.ac.kr)

The manuscript for this paper was submitted for review on April 30, 2005 / accepted on June 6, 2005

correspondence between the LIDAR points and their conjugate points from images.

2.1.1 Planar Patches from LIDAR data

Extracting planar patches from three-dimensional points of the LIDAR data has been proposed by Lee (2002). This approach is based on clustering of the LIDAR points with proximity and co-planarity. The main procedure is to establish adjacency among irregularly distributed three-dimensional points, to generate initial small patches (called seed patches) by clustering small number of points, and to grow iteratively the patches by sequentially adding the points adjacent to the growing patches. Each patch is then identified with its interior points, the plane parameters, and its boundary. Figure 1 shows an example of planar patches (b) segmented from LIDAR points (a). Among the segmented patches, the patches that are relatively smooth and large, and retain various slopes are actually selected for the registration. For examples, if only nearly horizontal patches are selected, the dependence among them may cause significant correlations between the estimates when estimating the exterior orientation parameters using the patches as control surfaces. In an extreme case in which all the segmented patches share almost the same slopes, a limited number of control points may be additionally required.

2.1.2 Conjugate Points from Images

Finding conjugate points from overlapping images has been conventionally implemented by deriving the relative orientation parameters between two images. The only difference from this conventional process is the selection of the locations of the conjugate points. In order to use conjugate points to register images with LIDAR data, it should be feasible to find their corresponding patches among the patches segmented from LIDAR data. For example, during the relative orientation, we often select the points located on building corners since those points are visually distinctive and well-defined. However, it might cause

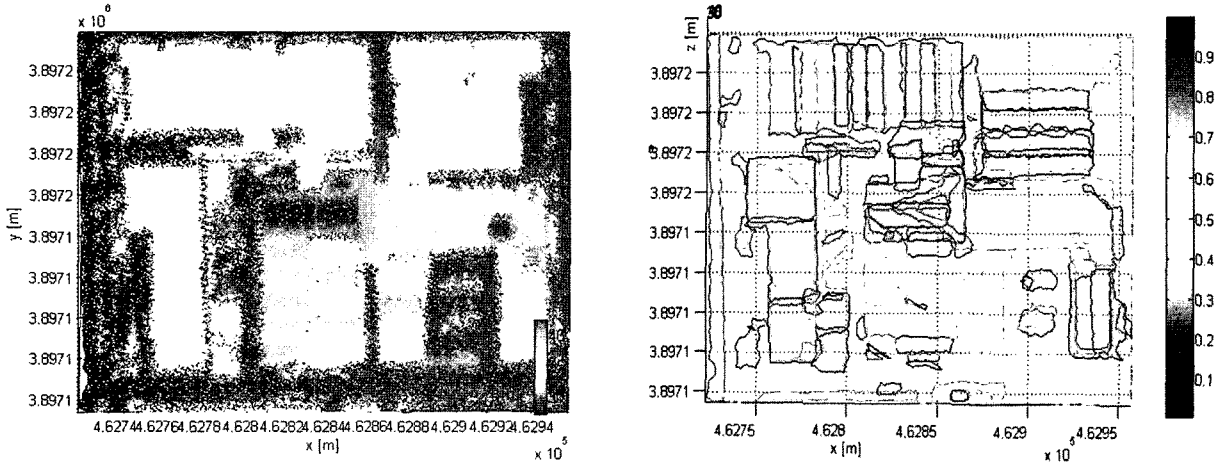

(a) The original LIDAR points (b) Segmented planar patches

Fig. 1. An example of planar patch segmentation from LIDAR points.

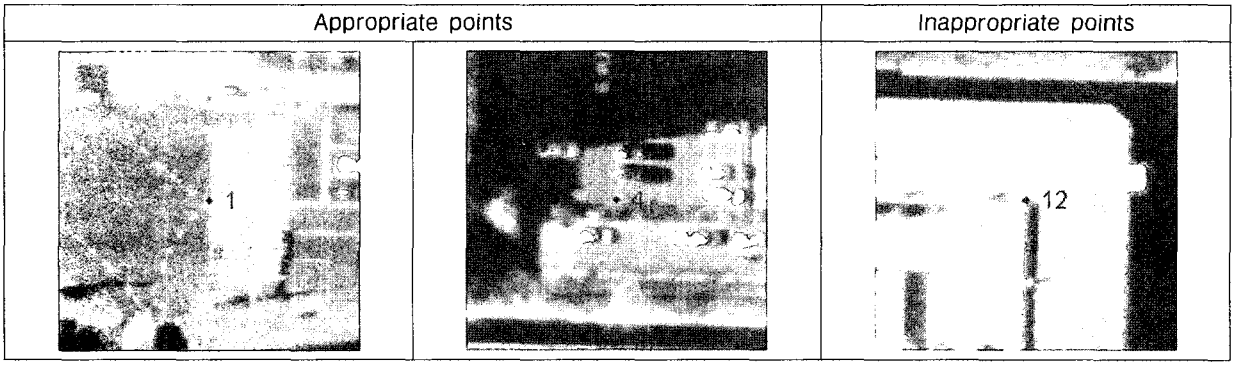

Fig. 2. Examples of appropriate and inappropriate tie points.

ambiguity problem in finding conjugate patches, if such points are selected, because there is a great possibility of existing more than one patch around the points. Hence, it is desirable to select the points on large planar surface that still show large variation of the brightness values. Without the geometric changes, this large variation can originate from radiometric changes, for examples, the intersections of white lines in parking lot or on roads. Fig. 2 shows examples of the both appropriate and inappropriate conjugate points.

2.2 Finding the Correspondence

After generating registration primitives individually from the image and point sets, it is attempted to establish the correspondence between the primitives. A three-dimensional point can be derived from each pair of the conjugate points with the initial approximations to exterior orientation parameters given by the GPS/INS module. Among the patches segmented from the LIDAR data, the nearest one to this point is then selected. If the distance from the selected patch to the specific point is within an error range, the patch is assigned to the corresponding patch to the pair of the conjugate points, as illustrated in Fig. 3. The range is determined by considering the positioning errors associated with the point, where these errors are roughly estimated by propagating the errors associated with the measurements about the conjugate points and approximation of the initial exterior orientation parameters.

2.3 Adjusting Exterior Orientation Parameters

With the registration primitives and their correspondence, the exterior orientation parameters are to be adjusted. In the ideal situation the ground point computed from a pair of conjugate points should exactly locate on its corresponding patch but this is rare in reality due to the errors associated with the acquisition of the images and LIDAR data. The systematic components of these errors mainly originate from the inaccurate exterior orientation parameters. These parameters are to be adjusted so that the differences between the ground points derived from the conjugate points and their corresponding patch will be minimized. This adjustment model is illustrated in Fig. 4.

The proposed adjustment model is different from the conventional one since it actually uses ground control surfaces rather than ground control points, where these control surfaces are the planar patches extracted from the LIDAR point set. Hence, this adjustment model employs the different mathematical equations from the conventional models, which are briefly summarized as follows.

Based on the principle of the central projection, the coordinates of an image point are determined by the co-linearity equations denoted as functions of the interior orientation parameters (I), the exterior orientation parameters (E), the coordinate vector of the ground point (P) represented in a ground coordinate system, as shown in Eq. (1).

$$p = f(I, E, P). \tag{1}$$

where p is the 2D coordinate vector for the image point represented in the image coordinate system.

Each pair of the conjugate points is corresponding to a planar patch represented as

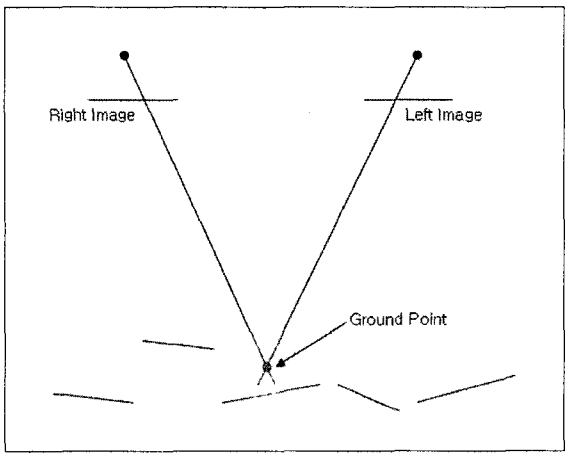

Fig. 3. Illustration of finding the patch corresponding to a pair of tie points.

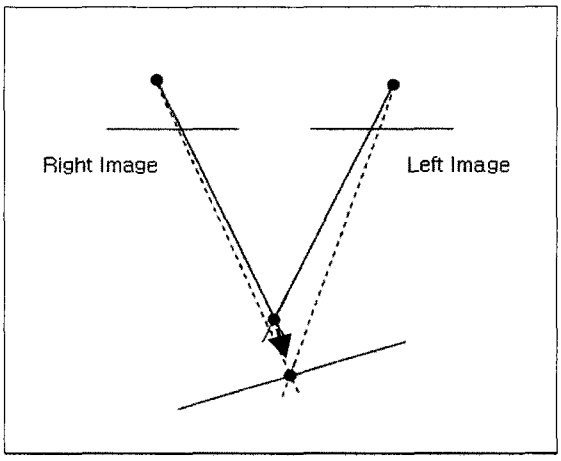

Fig. 4. The proposed adjustment model.

$$n \cdot P = d, \tag{2}$$

where n is the unit vector normal to the plane; P is the coordinate vector of any point on the plane, represented in a ground coordinate system; and d is the normal distance from the origin of the coordinate system to the plane.

Using the pairs of conjugate points, we establish the observation equations after linearizing the co-linearity equations and the stochastic constraints based on the corresponding patches as shown in Eq. (3) and (4).

$$p - f(I, E^*, P^*) = \frac{\partial f}{\partial E} \cdot \Delta E + \frac{\partial f}{\partial P} \cdot \Delta P + e_p, \tag{3}$$

$$d - n \cdot P^* = n \cdot \Delta P + e_c, \tag{4}$$

where E^* and P^* denote prior values of the exterior orientation parameters and the ground point coordinates, respectively; ΔE and ΔP represent updating unknown parameter vectors; e_p is the errors associated with the tie point measurement; e_c implies the uncertainty of the constraint mainly originating from the uncertainty of the plane parameters of the patch.

Since a patch provides a constraint expressed in Eq. (4), we need at least seven patches to provide the minimum seven independent ground control information which are required for the absolution orientation process that establish the relationship between an arbitrary selected model space and the object space. For example, let assume a LIDAR point set is located in the overlap area of the stereo image pair. Traditionally, in order to estimate the exterior orientation parameters of these images, we use six pairs of conjugate points, where the ground control points corresponding to three pairs among them are provided. If we perform this estimation with the patches, we need at least seven pair of conjugate points, each of which is assigned to its corresponding patch.

3. Experimental Results

The proposed approach has been applied to simulated data since the true values of the exterior orientation parameters and the ground point coordinates to be estimated are correctly known. The simulation procedure and the registration results are described in the following subsections.

3.1 Data Simulation

A pair of stereo-images obtained by an airborne wide-angle photogrammetric cameras was simulated. The focal length of the camera was assumed to be 153 mm and the dimension of the images to be 230 mm by 230 mm to depict aerial photos.

The exterior orientation of each image was assigned as shown in Table 1. The average terrain elevation and the flying altitude were assumed to be 0 m and 1530 m, respectively, to produce the photo scale of 1:10000. The ground coverage had more than 60% overlap as presented in Fig. 5. Each coverage boundary was generated using the exterior orientation parameters, the image size, and the average terrain elevation as assumed above. Twenty ground points were generated randomly inside the overlapping region. Their locations are also presented in Fig. 5. They were used to compute the true location of the tie points from each image. To simulate the measurement errors associated with the tie points, we then added a random noise to each tie point coordinate, where the standard deviation was ± 5 μm. The RMS values of the random noises actually added to x- and y-coordinates of the tie points of the left images were ± 6.3 μm and ± 4.6 μm, respectively. Those added to x- and y-coordinates of the tie points of the right images were ± 5.1 μm and ± 5.8 μm, respectively.

To simulate the biases associated with the given exterior orientation parameters, we also added some

Table 1. The true exterior orientation parameters

Item	Left Image	Right Image	Unit
Xc	1150	2070	m
Yc	0	0	m
Zc	1530	1530	m
κ	1	-1	deg
ϕ	-1	1	deg
κ	1	-1	deg

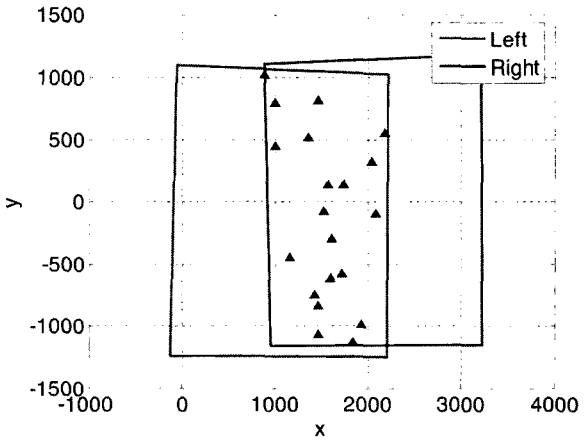

Fig. 5. Ground coverage and points.

systematic noises to the true exterior orientation parameters. The systematic noises were randomly generated with the standard deviations of ± 1 m and ± 0.01 deg for the three coordinates of perspective centers and the three rotational angles, respectively. These noisy parameters were then used as initial approximations in the registration process. The actual values are described in Table 2.

We then computed the ground points with the tie points and the exterior orientation parameters using the photogrammetric space intersection process. We determined true ground points using the true tie points and exterior orientation and then noisy ground points using noisy tie points and exterior orientation. The differences between the coordinates of the true ground points and noisy ones are shown in Fig. 6. The RMS values of these differences were ±5.48 m, ±9.30 m, and ±16.66 m in x-, y-, and z-coordinates, respectively.

Around each ground point, we generated a corresponding planar patch on which the point locates. The slopes of these patches were randomly selected as shown in Fig. 7.

To simulate LIDAR points, we randomly generated points on each patch. Each patch has different number of points as shown in Fig. 8. This simulates the different size of each patch. Random noises were then added to the points by considering the measurement

Table 2. The Noisy Exterior Orientation Parameters

Item	Left Image		Right Images		Unit
	Values	Noises	Values	Noises	
Xc	1156.76	6.76	2064.98	-5.02	m
Yc	1.62	1.62	0.87	0.87	m
Zc	1526.77	-3.23	1525.86	-4.14	m
κ	0.71035	-0.28965	-1.15904	-0.15904	deg
ϕ	-1.03625	-0.03625	0.98079	-0.01921	deg
κ	1.14750	0.14750	-1.14568	-0.14568	deg

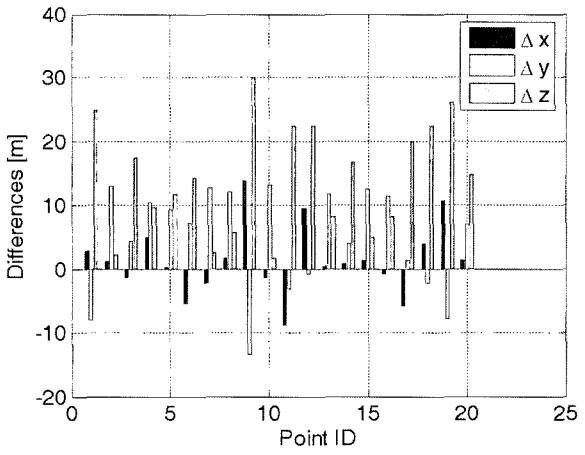

Fig. 6. The differences between the coordinates of the noisy ground points and the true ones.

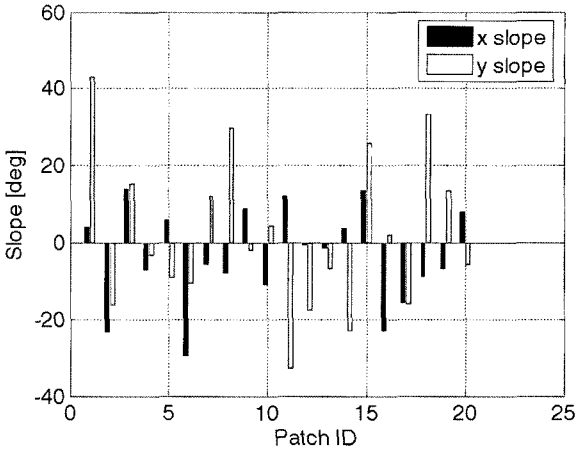

Fig. 7. The slopes of the patches in x- and y- directions.

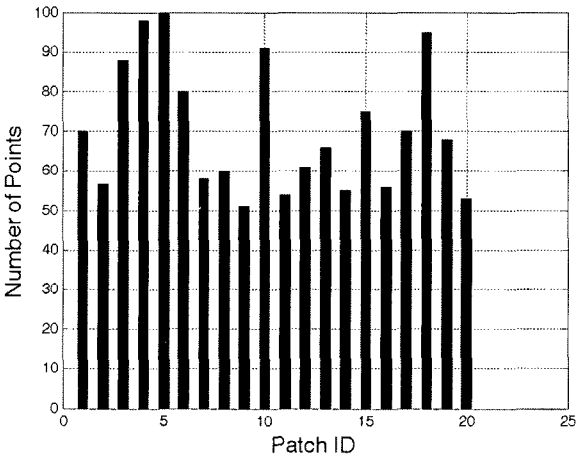

Fig. 8. Number of points generated on each patch.

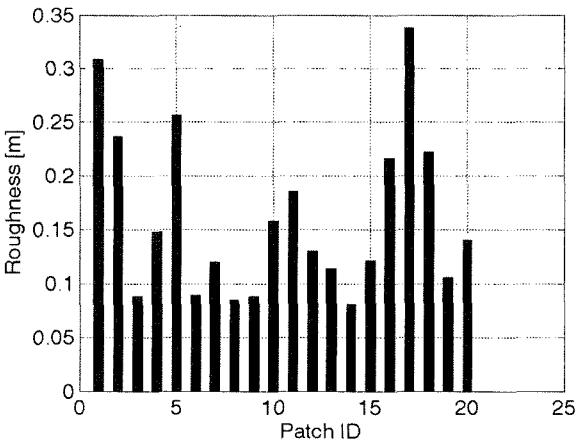

Fig. 9. Roughness of each patch.

errors of a LIDAR system and the roughness of the patch. The standard deviation used to generate the noises was differently assigned to each patch. By fitting a plane to these noisy points, we simulated planar patches segmented from LIDAR data. These patches have different roughness values as shown in Fig. 9. The RMS distance in z-direction from the true ground points to these noisy patches was about ± 0.061 m. That from the noisy ground points was about ± 17.433 m.

3.2 Registration Results

We established the observation equations to adjust the noisy exterior orientation parameters based on the noisy patches. Each pair of the tie points provides four collinearity equations; and each patch provides a

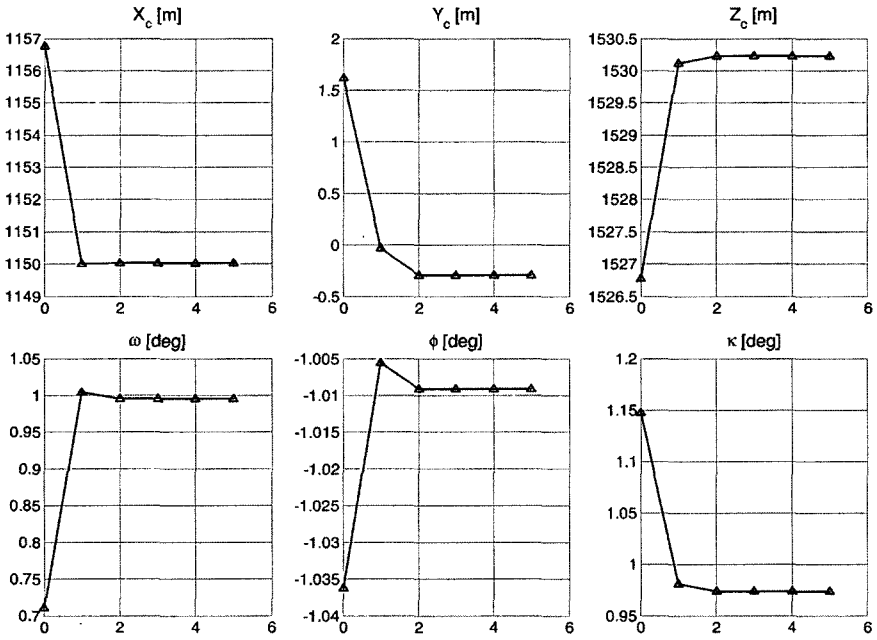

(a) Left Image

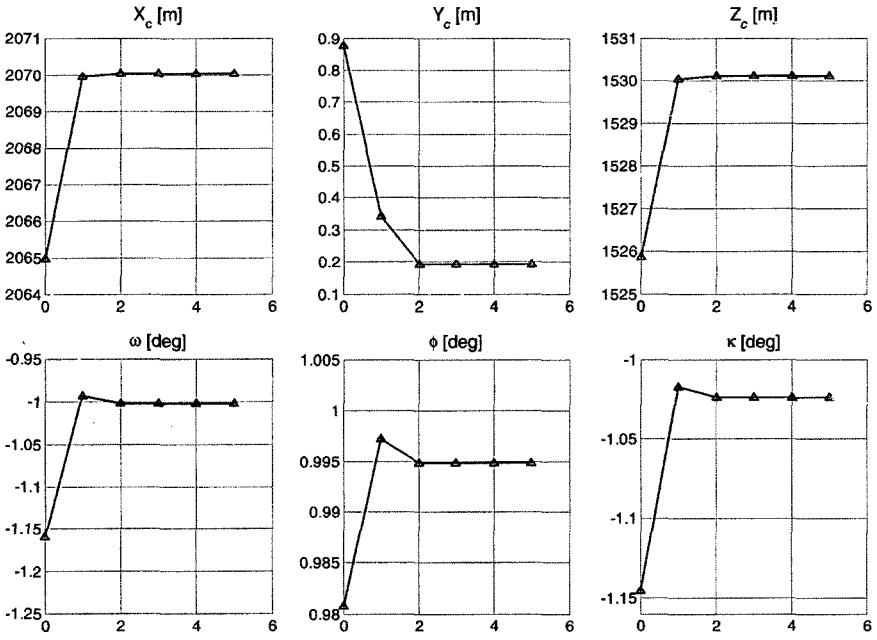

(b) Right Image

Fig. 10. Estimates for the exterior orientation parameters at each iteration step.

stochastic constraint. In total, we had 90 equations including the 10 constraints originating from the ground control information. If we assume no significant dependences between the equations, we can solve this system of the observation equations using the least squares method. The respective reciprocal of the variance of the noises added to tie points and the squares of the roughness of each patch were used as the weights of the observation equations.

Since the observation equations are non-linear, the adjustment process needs initial approximation and iterations. The estimates of the exterior orientation parameters of both images are determined with a few iteration steps as shown in Fig. 10. Within five iteration steps, the normal of the updates for the estimates decreased to less than the tolerance value specified to 10^{-9}. Table 3 presents the estimates for the exterior orientation parameters, the standard deviation of the estimates, and the differences from the true values described Table 2. As shown here, the exterior orientation parameters were precisely and accurately estimated. In addition, the correlations between the estimates were less than 0.7, which can be possible since the patches of various slopes as shown in Fig. 7 were used.

During the adjustment process, we generated the estimates for the ground points. As shown in Fig. 11, the differences between the estimated points and true ones are decreased within ± 0.8 m range. The RMS values of these differences are ±0.34 m, ±0.16 m, ±0.11 m in x-, y-, and z-coordinates, respectively. The RMS value of the distances in z-direction from the adjusted ground points to the control patches is about ±0.127 m.

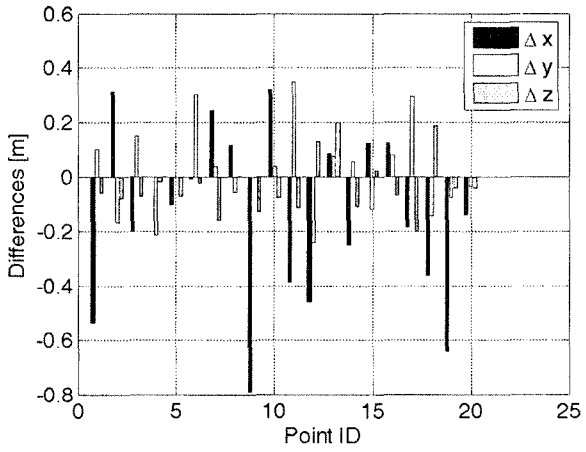

Fig. 11. The differences between the coordinates of the estimated ground points and true ones.

4. Conclusions

We proposed a method to precisely register images with LIDAR data by adjusting the exterior orientation parameters using the planar surface patches segmented from LIDAR data without any ground control point. Based on the experiment results with simulated data sets, it is shown that stereo images were registered to the LIDAR data with a RMS value of smaller than ±0.3 m. Further research is required to verify its performance by applying the proposed method to real data sets.

Table 3. Estimates for the exterior orientation parameters

Parameters		Estimates	Standard Deviation	Differences from the True Values	Unit
Left Image	Xc	1150.02	±0.54	0.02	m
	Yc	-0.30	±0.44	-0.30	m
	Zc	1530.22	±0.49	0.22	m
	κ	0.99516	±0.00960	-0.00484	deg
	ϕ	-1.00919	±0.01464	-0.00919	deg
	κ	0.97337	±0.03136	-0.02663	deg
Right Image	Xc	2070.03	±0.59	0.03	m
	Yc	0.19	±0.48	0.19	m
	Zc	1530.12	±0.48	0.12	m
	κ	-1.00224	±0.00920	-0.00224	deg
	ϕ	0.99483	±0.01475	-0.00517	deg
	κ	-1.02410	±0.03143	-0.02410	deg

Acknowledgement

We would like to thank the National Geographic Information Institute (NGII), Korea for supporting this research.

References

1. Habib, A.F., Ghanma, M.S., Morgan, M.F. and Mitishita, E. (2004). "Integration of Laser and Photogrammetric Data for Calibration Purposes." International Archives of Photogrammetry and Remote Sensing, 35(B2):170-175.
2. Habib, A. and Schenk, T. (1999). "New approach for matching surfaces from laser scanners and optical sensors." International Archives of Photogrammetry and Remote Sensing, 32(3W14):55-61.
3. Lee, I. (2002). Perceptual Organization of Surfaces, Ph.D. Dissertation, Dept. of Civil and Environmental Engineering and Geodetic Science, The Ohio State University, Columbus, OH.
4. Postolov, Y., Krupnik, A. and McIntosh, K. (1999). "Registration of airborne laser data to surfaces generated by photogrammetric means." International Archives of Photogrammetry and Remote Sensing, 32(3W14):95-99.
5. Schenk, T. and Csathó, B. (2002). "Fusion of LIDAR data and aerial imagery for a more complete surface description." International Archives of Photogrammetry and Remote Sensing, 34(3A):310-317.